Optimal Controller Gain Selection Using the Power Flow Information of Bond Graph Modeling

Robert T. McBride
Raytheon Missile Systems
P.O. Box 11337, Bldg. 805, M/S L-5
Tucson, AZ, 85734-1337, USA
rtmcbride@raytheon.com

François E. Cellier
University of Arizona
P.O. Box 210104,
Tucson, AZ, 85721-0104, USA
cellier@ece.arizona.edu

Keywords: Dymola, Modelica, object-oriented physical system modeling, graphical modeling, efficiency, optimization, autopilot gain selection.

Abstract

In the design of a controller, the selection of controller gains is the most time consuming and ad hoc of tasks. The difficulty lies in the fact that optimization tools cannot always find global optima, thus the solution found is more than likely sub-optimal. However, trying to find a more optimal solution quickly becomes cost ineffective. The controller gain selection process lacks a method for measuring the balance between 'good' and 'good enough'. The question of whether the controller gains need to be optimized further, or re-optimized in the instance of an existing design, often goes unanswered.

This paper is a companion paper to *System Efficiency Measurement through Bond Graph Modeling* [1]. In the companion paper, a method was shown, through the use of bond graphs, to evaluate the efficiency of a control scheme. This paper uses a similar method for evaluating the efficiency of controller gains for a given control system. The efficiency is used to define the optimal performance of the system. If the current set of controller gains is able to make use of the system's available energy, and these gains satisfy classical control criteria, then this set of gains is as close to the optimal solution as it needs to be. Further optimization would then be a waste of time and money, since the system performance cannot be improved. On the other hand, if the current set of gains does not make good use of the system's available energy, then the gains need to be optimized further.

INTRODUCTION

This paper shows, by means of an example, a method for selecting optimal controller gains by monitoring the power flow in a bond-graph model of the actuator. Here three sets of controller gains are compared, and an optimal set is selected.

This paper uses the servo-positioning system presented in the companion paper to control a two degree-of-freedom missile model. The controller discussion of the companion paper discussed primarily the control of the servo-system itself. Here the controller discussion focuses on an autopilot control of a missile system. The actuator control scheme, discussed in the companion paper, is buried inside the missile/autopilot system.

THE MISSILE MODEL

A missile model, autopilot, and actuation system are shown in figure 1. The modeling software used to create the models shown is Dymola [2]. Inside the block labeled *CAA_Fin1* is the same actuation system bond graph discussed in the companion paper. The bond-graph model of the actuation system has been dropped into this

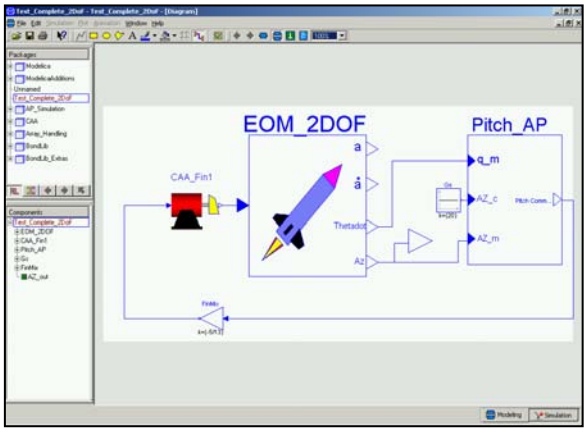

Figure 1. Missile System

block in an object-oriented fashion [3]. The controller used in the actuator for this paper is *controller 2*, as

described in the companion paper.

As seen in figure 1, the system is set up to command a 20 G step into the autopilot. The output of the system is the measured body acceleration of the missile.

The missile model shown in figure 1 is a two degree-of-freedom model. This model can be found in the book *Tactical and Strategic Missile Guidance* by Zarchan [4].

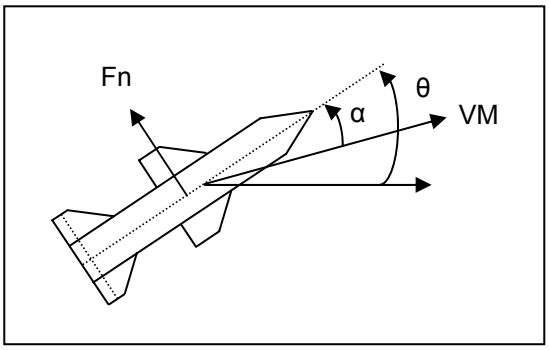

Figure 2. Two Degree-of-Freedom Missile

The two degrees of freedom, as described by figure 2, consist of a translational degree-of-freedom normal to the missile body, and a rotational degree-of-freedom about an axis coming out of the page. The normal force is described by equations 1-5.

$$m * A_z = Q * S_{ref} * C_N \tag{1}$$

$$Q = \frac{\rho * V_m^2}{2} \tag{2}$$

$$S_{ref} = \frac{\pi d^2}{4} \tag{3}$$

$$C_N = 2\alpha + \frac{1.5 * S_{plan} * \alpha^2}{S_{ref}} + \frac{8 * S_w * \alpha}{\beta * S_{ref}} + \frac{8 * S_T (\alpha + \delta)}{\beta * S_{ref}} \tag{4}$$

$$\beta = \sqrt{Mach^2 - 1} \tag{5}$$

where V_m is the missile velocity, S_{plan} is the planform area (approximated by the length of the missile * the diameter), S_{ref} is the missile reference area, S_w is the wing reference area, S_T is the tail reference area, α is the angle of attack, and δ is the tail deflection.

The moment equation is described by equations 6-7.

$$I_{yy} * \ddot{\theta} = Q * S_{ref} * d * C_M \tag{6}$$

$$\begin{aligned} C_M = {} & 2\alpha\left(X_{cg} - X_{CPN}\right) \\ & + \frac{1.5 * S_{plan} * \alpha^2}{S_{ref}}\left(X_{cg} - X_{CPB}\right) \\ & + \frac{8 * S_w * \alpha}{\beta * S_{ref}}\left(X_{cg} - X_{CPW}\right) \\ & + \frac{8 * S_T (\alpha + \delta)}{\beta * S_{ref}}\left(X_{cg} - X_{HL}\right) \end{aligned} \tag{7}$$

where X_{cg} is the distance from the nose to the center of gravity, X_{CPN}, X_{CPB}, and X_{CPW} are the distances from the nose to the centers of pressure for the nose, body, and wing, respectively, and X_{HL} is the distance from the nose to the hinge line of the missile. These distances are described graphically by figure 3.

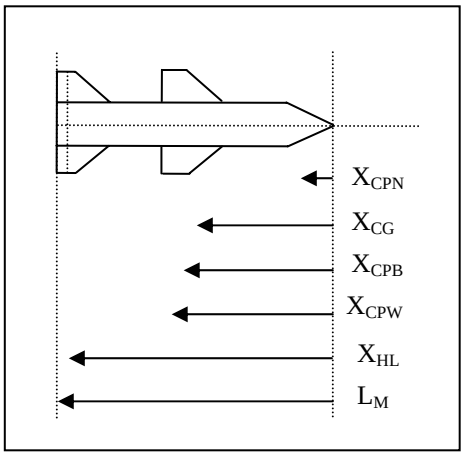

Figure 3. Missile Dimensions

The relationship between θ and α is

$$\dot{\alpha} = \dot{\theta} - \frac{A_z}{V_m} \tag{8}$$

As is seen by equations 1-8, the 2 degree-of-freedom missile is a non-linear set of ODE's. It would have been possible of course to describe the missile dynamics themselves by a bond graph, but this wasn't useful, as the

model provided is a standard model out of the open literature that is used commonly to describe missile dynamics. The model ensures that, for a given fin deflection, the missile will naturally adjust itself such that the moment coefficient, C_M, goes to zero. This is the trim condition for the given fin deflection. For C_M = 0, the value of α is non-zero. At the trim condition, the normal force is not zero, which provides the desired normal body acceleration.

Figure 4 shows the Dymola parameter window that defines each of the parameters of the model as used in this paper.

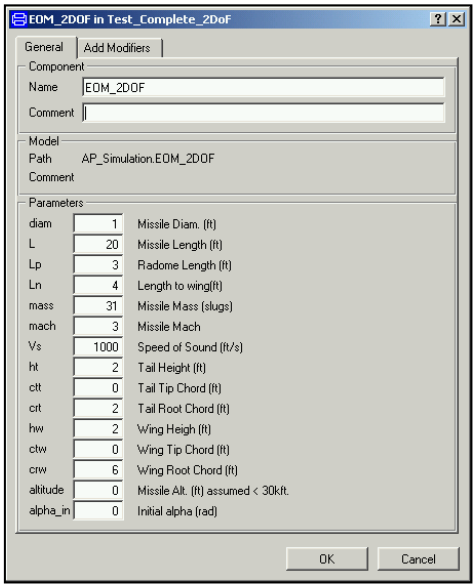

Figure 4. Missile Parameters

Figure 5 gives the meaning of the *tip* and *root chord* parameters shown in figure 4.

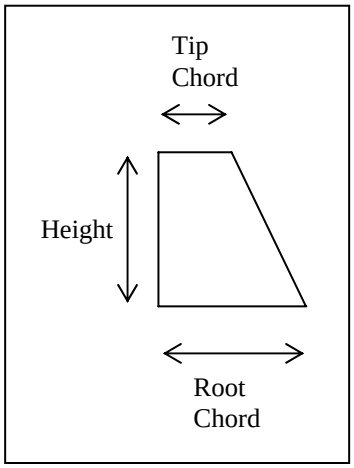

Figure 5. Wing Dimensions

Figure 6 shows the Dymola code used to implement the missile motion described by equations 1-8. The *der* function, shown in figure 6, is the Dymola notation for a derivative. This function is somewhat misleading in that there are no numerical derivatives calculated. The calculations are done through Dymola's ability to sort the equations horizontally, solve for the proper variables, and integrate where necessary [5].

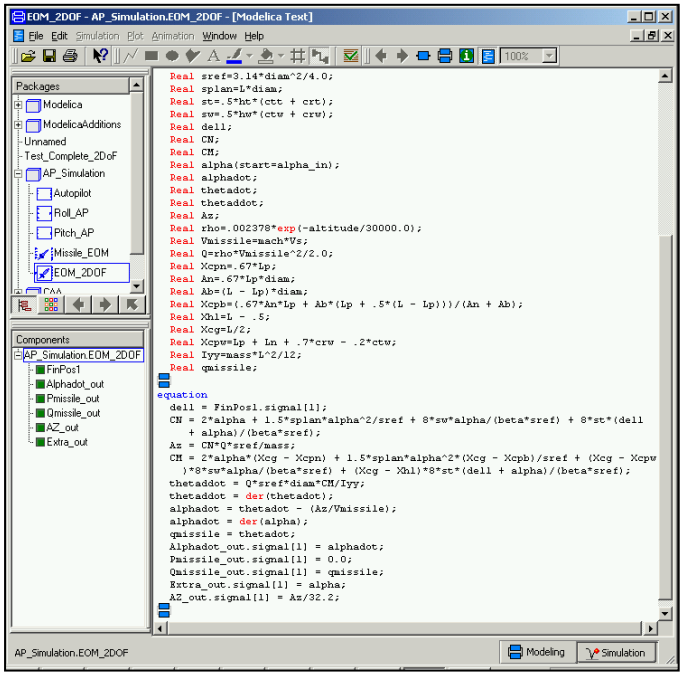

Figure 6. Missile 2 Degree-of-Freedom Code

The missile autopilot is shown in figure 7. The autopilot consists of an acceleration feedback path and two body-rate feedback paths used to help decouple the body acceleration from the pitch-rate.

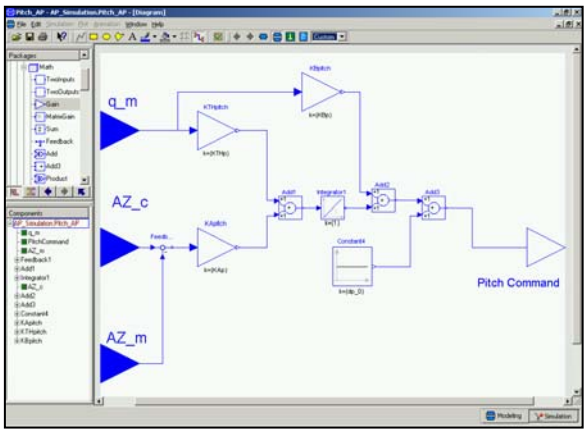

Figure 7. Pitch Autopilot

Figure 7 shows three gains in the autopilot control system, *KAp* in the integral feedback path, *KBp* in the cross-coupling feed-through path, and *KThp* in the cross coupling integral path. In the design of an autopilot, the selection of these controller gains is the most time consuming and ad hoc of tasks. The difficulty lies in the fact that optimization tools cannot always find global optima, thus the solution found is more than likely sub-optimal. Analyzing the power flow through the actuator, by monitoring the power flow in a bond graph, makes it possible to obtain an idea of the efficiency of a particular set of controller gains. Using this efficiency, a determination may be made on whether or not to continue searching for a more optimal set of controller gains, or stop the process and use the current set.

DYMOLA SIMULATION AND RESULTS

Simulation runs were preformed using three separate sets of controller gains as shown in table 1. These values produce the acceleration responses of figure 8. This figure is divided into two plots. The top portion shows the signals for the full simulation time, where the bottom figure is a zoom on the last second of simulation time to emphasize the differences in the run scenarios. As seen in figure 8, there is not much difference between the three scenarios. In the bottom plot of figure 8, scenario 1 is the middle signal, scenario 2 is the bottom signal, and scenario 3 is the top signal. Scenario 3 shows the largest steady state oscillation.

Run #	Kap	KBp	KTHp
1	1	0	1
2	1	0.125	0
3	1	0.125	2

Table 1. Gain Selections

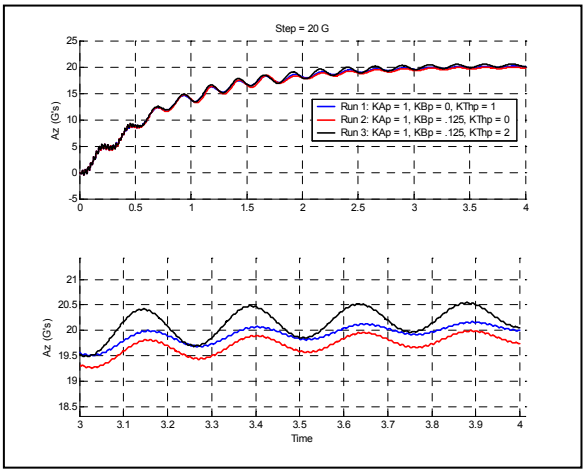

Figure 8. Achieved Acceleration (G's)

Figure 9 shows the achieved angle of attack for each of the three scenarios. As seen in figures 8 and 9, an angle of attack of 5.25 degrees results in 20 G's of missile acceleration.

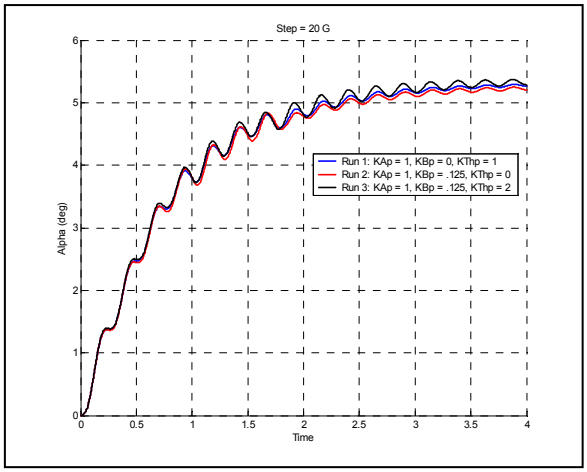

Figure 9. Achieved Angle of Attack

As in the companion paper, the input energy, which is the energy input from the bond-graph source, is compared to the output energy, which is the energy delivered to the fin. However, a slight variation of this calculation was used in this analysis. Here, the energy output to each of the bond-graph resistors was subtracted from the input energy. The reason this is done is to obtain an idea of efficiency that is similar to a thermodynamic idea of availability [6]. The energy lost to the resistors is not recoverable and is therefore not counted as usable energy. The efficiency calculated in this paper then compares the output energy to the energy available to the system, thus the irreversible energy does not influence the efficiency calculation.

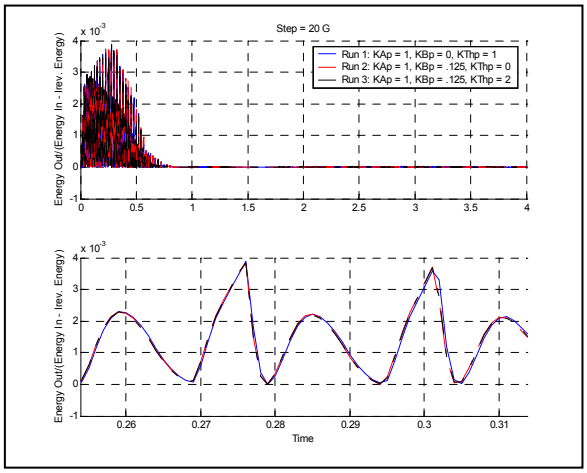

Figure 10. Output Energy/Available Energy

Figure 10 shows a plot of the energy output to the fin divided by the available energy. Similar to figure 8, figure 10 has been divided into two subplots, where the top portion shows an overall view of the time history, and the bottom portion shows a zoom on an area of interest. As seen in figure 10, even the zoomed in area, which includes the peak value of the response at 0.275 seconds, shows little difference in the responses.

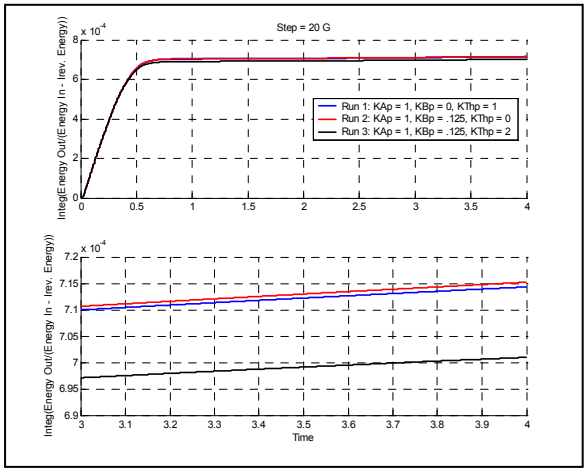

Figure 11. Integ (Output Energy/Available Energy)

Figure 11 is the integral of the signal shown in figure 10. This integration magnifies the differences between the three scenarios by continually summing up the signals of figure 10 over time. Run 1 is the middle signal, run2 is the top signal and run 3 is the bottom signal. Although the overall signals look similar, the zoom on the last second of the analysis shows that scenario 3 is not as efficient as scenarios 1 and 2 since, in scenario 3, less of the actuator's available energy is being used to control the missile. Scenarios 1 and 2 are similar enough to conclude that there is no reason to search further for a more optimal set of controller gains, among the three, since these two sets deliver nearly the same amount of energy to the fin. The gain sets of scenarios 1 and 2 are then judged as 'good enough'.

This paper compared three sets of controller gains to determine a suitable set. It was found that one set, scenario 3, was determined inefficient, where the other two sets are similar enough that they can be considered equivalent to each other. Of course, this doesn't tell us, whether there might exist other combinations of gain values that would be yet more efficient. Optimization techniques can be used to answer that question.

CONCLUSIONS

This paper shows, by means of an example of a two-degree of freedom missile simulation, a method, in which a bond-graph actuator model can be used to determine the efficiency of a set of controller gains. The bond-graph model maps the power flow through the actuator. The modeling software monitors the power flow through specific bonds of the actuator model. The energy delivered to the control surface is then normalized by the reversible energy in the system. This normalization provides a calculation of system efficiency. Based on the value of the efficiency signal, a set of controller gains is judged as inefficient or efficient enough to achieve the desired controller response.

This analysis provides a method for comparing the efficiency of controller gains that can be realized in a quick and affordable manner. Often parts procurement becomes an issue for aging systems. The introduction of new parts over time may eventually lead to the question of whether or not the current design is close to its optimum. If the gains of an existing control scheme are in doubt, as to whether or not more performance might be obtained in their re-optimization, then this analysis provides a method in determining the cost benefit of a controller re-design.

REFERENCES

[1] McBride, R.T. and F.E. Cellier (2005), "System Efficiency Measurement through Bond Graph Modeling," *Proc. ICBGM'05 Conference*, New Orleans, Louisiana.

[2] DYMOLA Dynamic Modeling Laboratory, World Wide Web page http://www.Dynasim.se.

[3] Cellier, F.E., and R.T. McBride (2003), "Object-Oriented Modeling of Complex Physical Systems Using the Dymola Bond-Graph Library," *Proc. ICBGM'03 Conference*, Orlando, Florida.

[4] Zarchan, P. (1997), "Tactical and Strategic Missile Guidance" Third Edition p. 461-469, *American Institute of Aeronautics and Astronautics, Inc.*

[5] Brück, D., H. Elmqvist, S.E. Mattsson, and H. Olsson (2002), "Dymola for Multi-Engineering Modeling and Simulation," *Proc. Modelica'2002 Conference*, Munich, Germany

[6] Cengel, and Boles (1989), "Thermodynamics: An Engineering Approach," *McGraw Hill*